

HIGH-FREQUENCY PROPERTIES OF THE ELECTRON FLOW SLOWING DOWN IN A PLANAR DIODE

*A.V. Pashchenko*², *O.G. Melezhik*¹, *S.S. Romanov*¹,
*D.A. Sitnikov*¹, *I.K. Tarasov*¹, *M.I. Tarasov*¹,
I.M. Shapoval^{1*}, *V.E. Novikov*², *V.A. Yatsyshin*³

¹*National Science Center "Kharkov Institute of Physics and Technology", 61108, Kharkov, Ukraine;*

²*Institute for Electrophysics and Radiation Technologies, National Academy of Sciences of Ukraine,
61002, Kharkov, Ukraine;*

³*Science-and-Production Center "Engineering-Technology Systems", 04210, Kiev, Ukraine*

(Received August 16, 2011)

The instability of the electron flow injected into a planar diode and slowed down in it under the action of the external electric field is investigated through the exact solution of the set of inhomogeneous hydrodynamic first-approximation equations of the stability theory. A dispersion equation has been derived, which relates the frequencies and increments (decrements) of arising electromagnetic oscillations to the parameters of the electron beam and the diode. The solution of the dispersion equation shows that in the diode, through which the slowing down electron beam is propagating, there arises the microwave oscillatory instability not described before. This instability occurs in the case when in the steady-state condition there is no potential minimum in the diode. The experiments have confirmed the occurrence of oscillatory instability with theoretically predicted frequencies and decrements in the corresponding beam and diode parameter regions.

PACS: 03.65.Pm, 03.65.Ge, 61.80.Mk

1. INTRODUCTION

It is commonly believed that all electromagnetic phenomena occurring in one of the simplest radiophysical devices, namely, the planar diode, have long been explored [1-4], and are the topics of education courses rather than the subjects of scientific research. However, it appears that a sequential development of theory (in particular, the application of Lagrangian description methods for electrodynamic processes) reveals a broad spectrum of new oscillation modes. The paper describes the new oscillation modes and instability, the existence of which has been corroborated by experiments.

In experimental physics, it is a currently accepted practice to determine high-frequency properties of volumes under vacuum in accelerators, magnetic traps, process devices, etc. In particular, experimental and theoretical efforts are aimed at determining the resonance properties of intrinsic cavities of experimental devices, the influence of cavity openings, branch pipes, projections, etc. on the excited spectra.

The knowledge of electromagnetic oscillations that may be excited in the setups is essential for understanding the behavior of accelerated/confined particles or plasma in the setups.

In this case, it is also of importance to determine

self-consistently the high-frequency properties of experimental setups with due regard for both the properties of accelerated/confined streams of particles or plasma and the geometry of vacuum chambers.

There are calculations made to date, which have resulted in the development of a great variety of electrodynamic devices for electromagnetic wave generation in different frequency ranges of particle accelerators and storage rings of various types, plasma confinement devices. However, a similar problem for the classical electrodynamic object, i.e., planar diode, still remained unsolved.

The authors of the present work have found the spectrum of electromagnetic oscillations, which can be excited in a planar diode on injection of the electron beam into it. It has been shown that in the case of electron beam deceleration in the diode there occurs a new (not described in the literature) instability, which is accompanied by excitation of the above-mentioned spectrum. Oscillations, which can be excited in a planar diode on injection of the electron beam into it. It has been shown that in the case of electron beam deceleration in the diode there occurs a new (not described in the literature) instability, which is accompanied by excitation of the above-mentioned spectrum.

*Corresponding author E-mail address: shapoval@kipt.kharkov.ua

2. CHOICE OF THE ELECTRON-FLOW MODEL

In our studies the electron flow in the diode is considered in the one-dimensional hydrodynamic approximation. Fig.1 shows the electrode geometry and the qualitative potential distribution pattern in the diode.

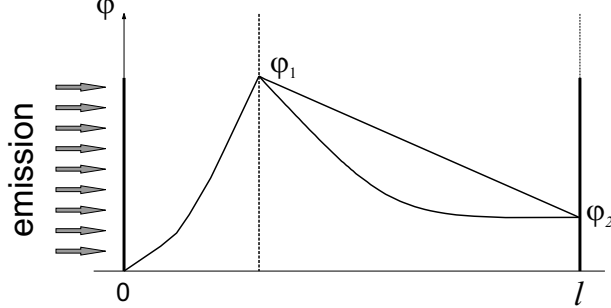


Fig.1. The qualitative distribution pattern in the triode

The qualitative conclusions of the one-dimensional model used here hold true in two-dimensional models, too, though a detailed behavior of the flow changes when passing from one- to two-dimensional problems.

The one-dimensional hydrodynamic equations of motion and continuity as well as the Poisson equation for the electric field are the initial equations:

$$\begin{aligned} \frac{\partial v}{\partial t} + v \frac{\partial v}{\partial z} &= \frac{\partial \Phi}{\partial z}, \\ \frac{\partial n}{\partial t} + \frac{\partial}{\partial z}(nv) &= 0, \\ \frac{\partial^2 \Phi}{\partial z^2} &= qn. \end{aligned} \quad (1)$$

The equation of motion is, in effect, the second Newton's law for a macroscopically small volume of the electron flow. The hydrodynamic equation of continuity expresses the particle conservation law. In the Coulomb gauge the scalar potential $\hat{\Phi}$ is determined by the charge distribution.

The input flow parameters of the diode, namely, n_0 , v_0 ; the diode gap width l and the time of flow transit of the distance l at a velocity v_0 , are the units of measurement of density n , velocity v , coordinate z and time t . The dimensionless electric-field potential $[\Phi] = \frac{mv_0^2}{e}$ is the ratio of the double kinetic energy of the flow to the electric field energy, $q = 4\pi e^2 n_0 l^2 / mv_0^2$.

3. STEADY-STATE CONDITIONS OF THE ELECTRON FLOW. LAGRANGIAN FORMALISM

We write the time- and coordinate-dependent quantities as follows

$$\begin{aligned} v(z, t) &= v^0(z) + \tilde{v}(z, t), \\ n(z, t) &= n^0(z) + \tilde{n}(z, t), \end{aligned} \quad (2)$$

$$\Phi(z, t) = \Phi^0(z) + \tilde{\Phi}(z, t),$$

where $v^0(z)$, $n^0(z)$, $\Phi^0(z)$ are the stationary quantities.

The relations describing the current density stability and the flow energy conservation law are the stationary solutions of the system (1):

$$\begin{aligned} n^0(z)n^0(z) &= 1, \\ \varphi(z) &= \frac{1}{2} - \frac{v^0(z)^2}{2}. \end{aligned} \quad (3)$$

Let us consider the slowing down flow, i.e., the potential of the second electrode is negative, $\Phi_l < 0$ ($\Phi^0 = -\varphi$, $\varphi > 0$). With the use of integrals (3), the solution of the problem for the steady-state conditions leads to the following relations:

$$\frac{1}{3}(v^0 + c)^{\frac{3}{2}} - c(v^0 + c)^{\frac{1}{2}} = -\sqrt{\frac{q}{2}}(z - \bar{z}). \quad (4)$$

The constants c and z are determined from the boundary conditions

$$v^0(z=0) = 1, \quad v^0(z=l) = v_l, \quad v_l = \sqrt{1 - \varphi_l}.$$

$$(v_l + c)^{\frac{1}{2}} \cdot (-v_l + 2c) - (1 + c)^{\frac{1}{2}}(-1 + 2c) = \sqrt{\frac{9}{2}}q, \quad (5)$$

$$\begin{aligned} \bar{z} &= \frac{1}{2} - \frac{1}{3\sqrt{2}q}[(v_l + c)^{\frac{1}{2}} \cdot (-v_l + 2c) - \\ &\quad -(1 + c)^{\frac{1}{2}}(-1 + 2c)]. \end{aligned} \quad (6)$$

Equation (6) defines the coordinates of the plane, where the flow rate is equal to c (5). We introduce the Lagrange time τ . Then by definition we have $v^0(z) = \frac{dz}{d\tau}$, and both the rate of the stationary flow and its coordinate are given by the following relations, depending on τ and the parameters of flow and diode:

$$\begin{aligned} v^0(\tau) &= \frac{q}{2} \left(\tau - \frac{1}{\sqrt{q\gamma}} \right)^2 + 1 - \frac{1}{2\gamma}, \\ z &= \frac{q}{6} \tau^3 - \frac{1}{2} \sqrt{\frac{q}{\gamma}} \tau^2 + \tau, \\ c &= \frac{1}{2\gamma} - 1. \end{aligned} \quad (7)$$

Since $|c| \leq 1$, then we have $\infty > \gamma \geq 1/4$. Equation (5) that defines c can be rewritten as

$$q(\gamma, v_l) = \frac{1}{\gamma} \left[1 - \frac{1}{3\gamma} + \right]$$

$$+\frac{1}{3}(-v_l + \frac{1}{\gamma} - 2)\sqrt{1 - 2\gamma(1 - v_l)}]^2, \quad (8)$$

and the coordinate of the plane, where the flow rate is equal to c , is written as

$$\bar{z} = \frac{1}{2} - \frac{1}{2\sqrt{q\gamma}}[-1 + \frac{1}{3\gamma} + \frac{1}{3}(-v_l + \frac{1}{\gamma} - 2)\sqrt{1 - 2\gamma(1 - v_l)}]^2. \quad (9)$$

For example, for the drift space at $\gamma=1$ and $v_l=0.5$ we obtain $q=4/9$ and $z=1$. Note that the gap transit time ($z = z_l = 1$) for the stationary flow is equal to

$$\tau_l = \frac{1}{\sqrt{q\gamma}}(1 + \sqrt{1 - 2\gamma(1 - v_l)}). \quad (10)$$

4. DEVIATIONS FROM THE STATIONARY STATE

We assume the deviations from stationary values to be small and consider a linearized set of equations (1). According to expression (2) we have

$$\begin{aligned} -i\omega\tilde{v}(z) + \frac{d}{dz}[v_0(z)\tilde{v}(z)] &= -\frac{d\Phi^0}{dz}, \\ -i\omega\tilde{n}(z) + \frac{d}{dz}[n^0(z)\tilde{v}(z) + \tilde{n}(z)v^0(z)] &= 0, \\ \frac{d^2\Phi^0(z)}{dz^2} &= -q\tilde{n}(z). \end{aligned} \quad (11)$$

The time dependence of deviation variables is proportional to $e^{-i\omega t}$ and from here on the tilde over the deviation terms will be omitted. From expression (11) we obtain the following equation:

$$\begin{aligned} [v^0(z)]^3 \frac{d^2u}{dz^2} + qu &= \\ = C_1[v^0(z)]^2 \exp(-i\omega \int_0^z \frac{dx}{v^0(x)}), \end{aligned} \quad (12)$$

where $u(z) = v^0(z)\exp(-i\omega \int_0^z \frac{dx}{v^0(x)})$, and C_1 is the integration constant proportional to the Fourier amplitude being the total current component. Eq. (11) is solved in terms of Lagrange variables. Using the relations derived, we rewrite eq. (12) as

$$v^0(\tau) \frac{d^2u}{d\tau^2} - \frac{dv^0(\tau)}{d\tau} \frac{du}{d\tau} + qu = C_1[v^0(\tau)]^2 e^{-i\omega\tau}. \quad (13)$$

With the known solution of the homogeneous equation, i.e., eq. (13), where the right-hand member equals zero, and using the method of variation of arbitrary constants we find the following solution

$$\begin{aligned} u(\theta) &= (\theta - 1)D_1 + D_2[\theta(\theta - 1) + 1 - 2\gamma] + \\ &+ C e^{-\sigma\theta}[1 - 2\gamma - \frac{2}{\sigma}(\theta - 1) - (\theta - 1)^2]. \end{aligned} \quad (14)$$

In relation (14), the Lagrange variable is denoted as $\theta = \tau\sqrt{q\gamma}$, the parameter σ is given by $i\omega/\sqrt{q\gamma}$, $C = -C_1/2\sigma^2q\gamma^2$, D_1 and D_2 are the integration constants. Going in eq.(11) from z to θ we obtain the following formula

$$\varphi(\theta) = \varphi(0) + \int_0^\theta dx \frac{du}{dx} e^{\sigma x}. \quad (15)$$

The substitution of the velocity disturbance (14) into formula (15) results in

$$\begin{aligned} \varphi(\theta) &= \varphi(0) - \frac{D_1}{\sigma}(e^{\sigma\theta} - 1) - \\ &- \frac{D_2}{\sigma}[e^{\sigma\theta}(2\theta - \frac{2}{\sigma} - 1) + 1 + \frac{1}{\sigma}] + \\ &+ C\sigma(1 - 2\gamma + \frac{2}{\sigma^2}\theta - \frac{(\theta - 1)^3 + 1}{3}). \end{aligned} \quad (16)$$

The density deviation from the stationary value can now be found by eq. (15) as

$$\begin{aligned} n(\theta) &= \frac{\gamma}{[v^0(\tau)]^2}(D_1 e^{\sigma\theta}[\sigma - \frac{\theta - 1}{\gamma v^0}] + \\ &+ D_2 e^{\sigma\theta}[2\sigma\theta + 2 - \sigma - \frac{\theta - 1}{\gamma v^0}]) + \\ &+ C\sigma[(2\theta - 1) - \frac{\theta - 1}{\gamma v^0}(-1 + 2\gamma + (\theta - 1)^2 - \frac{2}{\sigma^2})]. \end{aligned} \quad (17)$$

5. FREQUENCY SPECTRUM OF SPACE-CHARGE WAVES

The integration constants in eqs. (15)-(17) are found with the help of the boundary conditions (18)

$$\begin{aligned} v(z=0) &= 0, \quad n(z=0) = 0, \\ \varphi(z=0) &= 0, \quad \varphi(z=1) = 0. \end{aligned} \quad (18)$$

The conditions imply that at the diode input there are no deviations of hydrodynamic quantities from their stationary values. Similarly, at the diode output there is no deviation of the potential from its stationary value. That is to say, to a first approximation, nothing from the outside is brought into the diode, and at the output the system responds in a self-consistent way. The third condition in (18) is satisfied by itself. The first, second and fourth conditions form a homogeneous system for the unknown quantities D_1, D_2, C :

$$\begin{aligned} D_1 - D_2(1 - 2\gamma) + 2C(\gamma - \frac{1}{\sigma}) &= 0, \\ D_1(1 + \frac{1}{\gamma\sigma}) + D_2(\frac{2}{\sigma} - \frac{1}{\gamma\sigma} - 1) - C \cdot \frac{2}{\gamma\sigma^2} &= 0, \\ D_1(e^{\sigma\theta_l} - 1) + D_2[e^{\sigma\theta_l}(2\theta_l - \frac{2}{\sigma} - 1) + 1 + \frac{2}{\sigma}] &+ \end{aligned}$$

$$+C\sigma^2\left[(-1+2\gamma-\frac{2}{\sigma^2})\theta_l+\frac{(\theta_l-1)^3+1}{3}\right]=0. \quad (19)$$

This system has non-zero solutions when the determinant composed of the coefficients of the unknowns is equal to zero.

The calculations lead to the following equation for the frequency spectrum of space-charge waves, which can exist in the diode at conditions of no particle reflection, when the potential minimum is absent:

$$e^{2\alpha}(1-\alpha)+4G\alpha^3-\alpha-1=0. \quad (20)$$

Here we introduced the notation

$$2\alpha = \sigma\theta_l,$$

$$G = \frac{-1+2\gamma(v_l+2)-\sqrt{1-2\gamma(1-v_l)}}{6[1+\sqrt{1-2\gamma(1-v_l)}]^2}. \quad (21)$$

To find the complex roots (20), we put

$$\sigma = -Q + iP. \quad (22)$$

So, in accordance with the notation introduced, we have

$$\omega = \sqrt{q\gamma}(P + iQ). \quad (23)$$

The time dependence is given as $e^{-i\omega t}$, therefore at $Q > 0$ the instability takes place, and at $Q < 0$ we have the stability. From eq. (20), after substitution of (22) and separation of imaginary and real parts, we obtain the following equations

$$4G = \frac{e^{-2Q}[(1+Q)\cos 2P + P\sin 2P] + Q - 1}{Q(Q^2 - 3P^2)}, \quad (24)$$

$$4G = \frac{e^{-2Q}[(1+Q)\sin 2P + P\cos 2P] - P}{P(P^2 - 3Q^2)}. \quad (25)$$

Equations (24), (25) enable us to find $P(q, v_l)$ and $Q(q, v_l)$. Their plots are presented in Figs.1 and 2.

The first five solutions of eqs. (24), (25) indicate that with an increase in q stationary states set in. Their frequency is proportional in the order of magnitude to the electronic Langmuir frequency (see Fig.2).

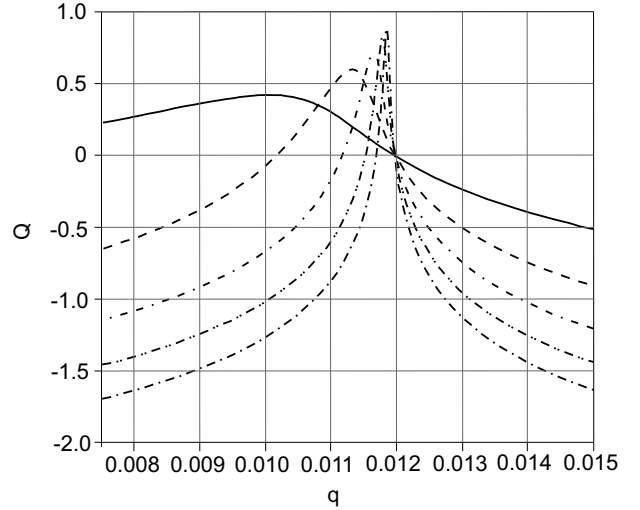


Fig.2. Oscillation increments at $V_l = 0.8$

The range of q values, where $Q > 0$ is rather narrow. For example, in Fig.1, at $q=0.0115$ we have $Q=0.5$. $Q > 0$ case corresponds to the onset of the instability, and the $Q < 0$ case corresponds to the damping of arising oscillations.

The oscillation increments for $Q > 0$ (see Fig.2) have their maximum values for a wide frequency range in the narrow parameter q region in the neighborhood of zero. The oscillation spectrum, which can be excited in the diode, presents a set of discrete frequencies. This permits the excitation of both the oscillations with dedicated frequency and a set of oscillations. The oscillation frequencies and oscillation increments can be found by multiplying P and Q by the dimension factor $\frac{v_0}{l}\sqrt{q\gamma}$. As it can be seen in Fig.3, the increment of instability Q takes on small values ($Q \approx 0.5 \dots 0.7$), which prevent the instability from causing the beam breakup during the transit time.

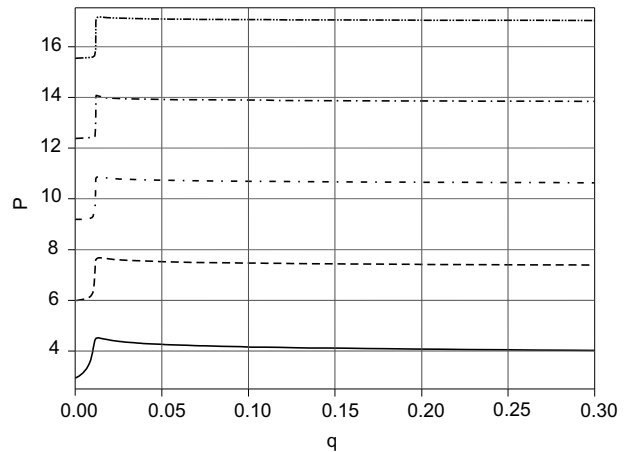


Fig.3. Frequencies at $V_l = 0.8$

The analysis of the dispersion equation has enabled us to determine the parameter regions (q and V_l), where the oscillations get excited at the expense of the instability under study (Fig.4).

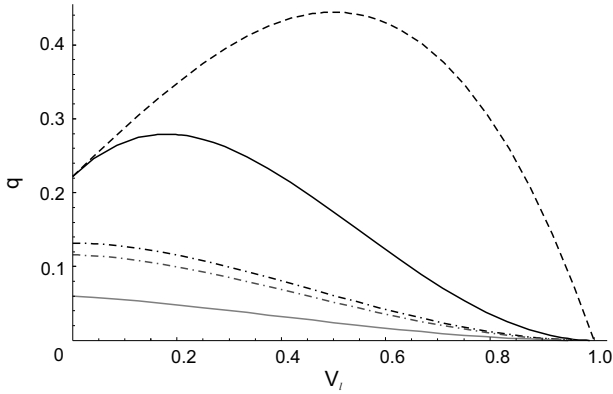


Fig.4. Excitatory regions of the first and second frequency bands

Curves 1 in Fig.4 define the excitatory region of the first frequency band (lower curve in Fig.2). Curves 2 define the region for the second frequency band. As it can be seen from the figure, the instability is observed in a rather narrow range of small q values.

6. EXPERIMENTAL STUDIES OF INSTABILITY OF ELECTRON-BEAM STATIONARY STATES IN THE DIODE

The electron beam instability was found and investigated experimentally at the devices, which simulated the conditions of the instability onset defined by theoretical calculations. The electron flow was investigated in a planar triode electrode geometry. The experimental arrangement is presented in Fig.5.

The electron flow produced by the indirectly heated cathode 1 propagated towards anode 3 and grid 2. The linear dimensions of the electrodes (grid, anode) substantially exceeded the interelectrode spacing. The cathode-grid and grid-anode separation distances are in the ratio of 1:5.

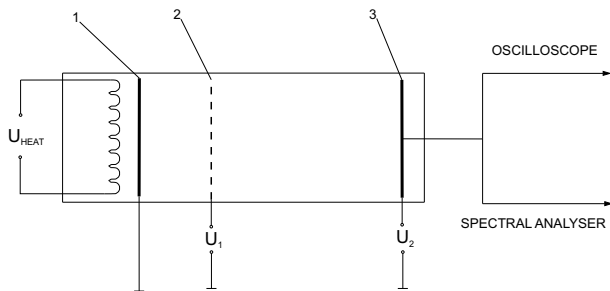


Fig.5. Schematic of the experimental arrangement.
1 - indirectly heated cathode, 2 - grid, 3 - anode

In the experiments, we have measured such parameters as the anode/grid voltages (U_1 and U_2), and also the emission current density and the oscillation spectrum. The amplitude of oscillations was also measured, and the increments were estimated.

In the first case, the vacuum chamber, in which the experiments were performed, was pumped down to a residual pressure of $\sim 2 \times 10^{-6}$ Torr.

In the second case, when the vacuum chamber was operated, the residual pressure was estimated to be about $\sim 10^{-7}$ Torr. In both cases, the potentials were applied to the grid and the anode relative to the grounded cathode.

Based on the measurements of the emission current for different potential values at the grid and the anode, we have plotted the voltage-current characteristics of the grid-anode distance (Fig.6).

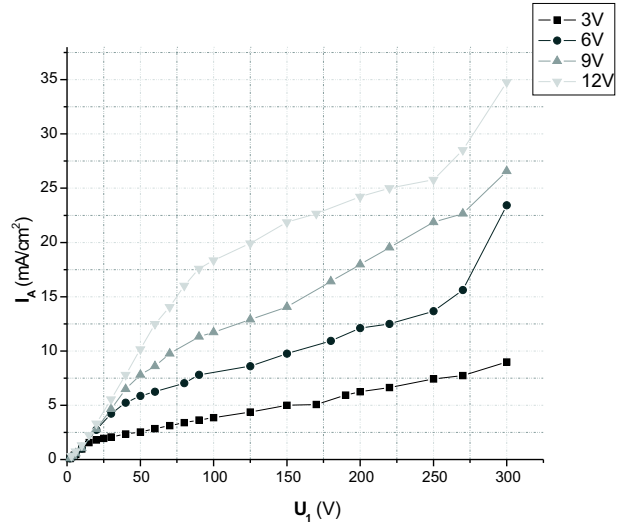


Fig.6. Voltage-current characteristics of the grid-anode distance for different anode potential values

The instability was detected and observed only in the case when the potential applied to the grid was in excess of the anode potential. This corresponds to the mode of beam slowing-down in the diode.

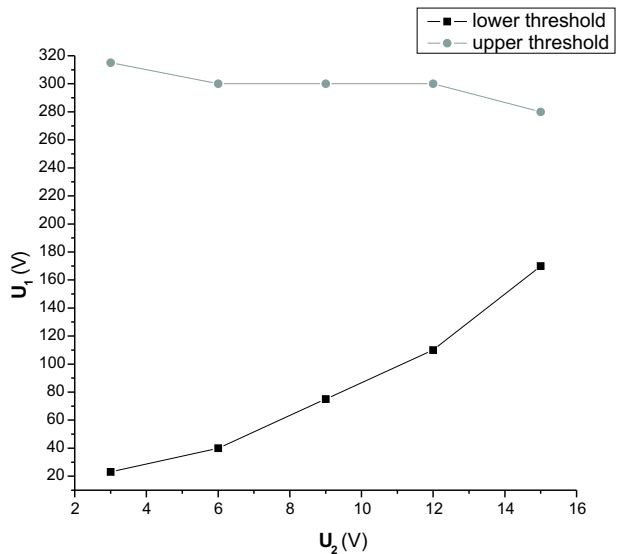


Fig.7. Upper and lower thresholds of oscillation excitation

The process of excitation had a threshold character in relation to the grid/anode potential values. The threshold values of anode/grid potentials are presented in Fig.7.

The excitation of oscillations takes place in the region bounded by the curves shown in Fig.7.

The treatment of these and similar curves provides the comparison between the experimental data and the theoretical predictions.

The measurements and the analysis of the experimental data have demonstrated that the excitation of oscillations takes place in the q and v_i parameter region predicted by theory, this being confirmed by the data presented in Fig.8.

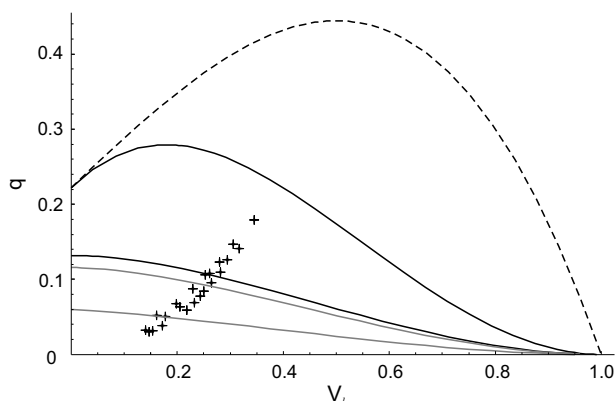


Fig.8. Regions of oscillation excitation and the points, at which the instability was observed experimentally

In Fig.8, the points corresponding to the experimental measurements are plotted against the background of the theoretical curves bounding the regions of oscillation excitation. Each point presents a set of parameters, at which the excitation of oscillations was observed.

The frequencies were measured with the help of the spectrum analyzer. In the process of measurements the frequencies of the first and second frequency bands were recorded. In some modes of operation, the excitation of the third frequency band could also be observed.

For comparison between experimental and theoretical results, Fig.9 shows the points obtained from the oscillation frequency measurements at different grid/anode potentials against the theoretical boundaries of oscillation P-excitation bands. It can be seen that with an increase in the anode potential the ratio of the points falling in the band indicated by theory to those lying beyond the band changes in favor of the first ones. At the anode voltage $U_2 = 3V$ their number makes 50% of the total number of points, 71.4% and 100% at $U_2 = 6V$ and $U_2 = 9V$, respectively. So, it can be stated that with a further going into the mode of slowing down (from the reflection mode) the agreement between the experimental and theoretical results is considerably improved.

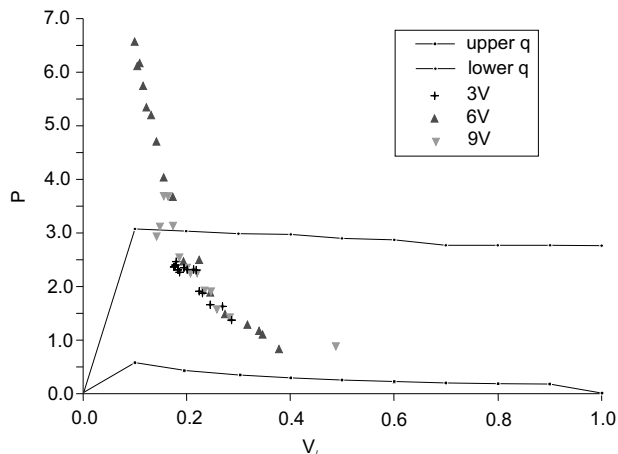


Fig.9. P excitation band boundaries obtained theoretically (solid lines) and frequencies observed experimentally at different anode potentials (points)

The mode shape was investigated with the help of a high-speed oscillograph. The amplitude of oscillations was registered at different moments of time as the instability under study was developing.

As a result of multiple studies of the mode shape during instability excitation, a number of increments of growth were obtained for different stages of instability development. Based on the results obtained, average increments of growth of the amplitude of oscillations were estimated at different q values.

Figure 10 gives the values of increments obtained experimentally against the curves resulting from the theoretical study of the instability.

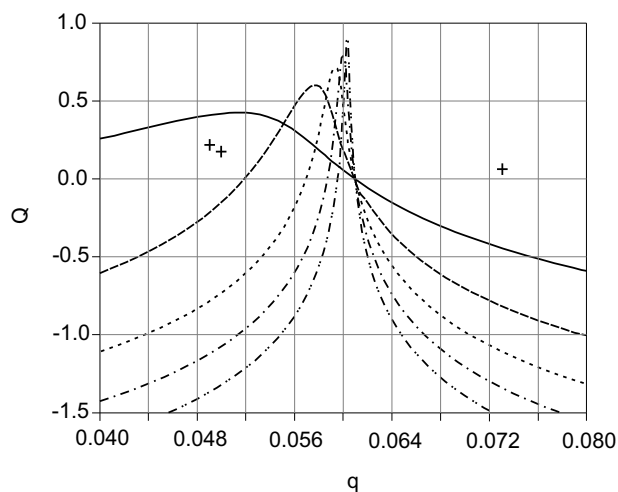


Fig.10. Comparison of experimental increments of instability growth (crosses) with theoretical predictions for different q at $v_i = 0.5$

7. CONCLUSIONS

The instability of accelerated and slowed down beams has been investigated in the mode without the potential minimum. For slowed down beams, the

instability has been revealed, which corresponds to small parameter q values. The instability can be interpreted as a linear stage of transition from a quasi-single-particle mode of beam propagation to the hydrodynamic mode.

Experiment has been performed to detect and investigate the instability. The experiment has confirmed the occurrence of the instability in the region of parameters predicted by theory.

References

1. A.V.Pashchenko, B.N.Rutkevich. The stability of electron flow in diode // *Plasma Physics*. 1977, v.3, p.774.
2. R.B.Miller. *Intense charged particle beams*. "Plenum Press", New York and London: 1982, 432 p.
3. I.I.Magda, V.E.Novikov, A.V.Pashchenko, S.S.Romanov, I.M.Shapoval. To the theory of beam feedback in the generators with a virtual cathode // *VANT*. 2003, v.6, N46, p.167-170.
4. J.Pierce. Limiting stable current in electron beams in the presence of ions // *J. Appl. Phys.* 1944, v.15, p.721.

ВЫСОКОЧАСТОТНЫЕ СВОЙСТВА ЭЛЕКТРОННОГО ПОТОКА, ЗАМЕДЛЯЮЩЕГОСЯ В ПЛОСКОМ ДИОДЕ

*А.В. Пащенко, О.Г. Мележик, С.С. Романов, Д.А. Ситников, И.К. Тарасов,
М.И. Тарасов, И.Н. Шаповал, В.Е. Новиков, В.А. Яццилин*

На основе точного решения системы неоднородных гидродинамических уравнений первого приближения теории устойчивости изучена неустойчивость электронного потока, который инжектирован в плоский диод и замедляется в нём под действием внешнего электрического поля. Получено дисперсионное уравнение, связывающее частоты и инкременты (декременты) возникающих электромагнитных колебаний с параметрами электронного потока и диода. Решение дисперсионного уравнения показывает, что в диоде, через который распространяется замедляющийся электронный поток, возникает не описанная ранее неустойчивость колебаний в СВЧ-диапазоне. Эта неустойчивость имеет место, когда в стационарном состоянии минимум потенциала в диоде не образуется. Экспериментально подтверждено возникновение неустойчивости колебаний с предсказанными теоретически частотами и декрементами в соответствующих областях параметров пучка и диода.

ВИСОКОЧАСТОТНІ ВЛАСТИВОСТІ ЕЛЕКТРОННОГО ПОТОКУ, СПОВІЛЬНЕНОГО У ПЛОСКОМУ ДІОДІ

*А.В. Пащенко, О.Г. Мележик, С.С. Романов, Д.А. Ситников, И.К. Тарасов,
М.И. Тарасов, И.М. Шаповал, В.Е. Новіков, В.А. Яццилин*

На основі точного рішення системи неоднорідних гідродинамічних рівнянь першого наближення теорії стійкості вивчена нестійкість електронного потоку, інжектованного у плоский діод і сповільненого в ньому під дією зовнішнього електричного поля. Отримано дисперсійне рівняння, що пов'язує частоти і інкременти (декременти) виникаючих електромагнітних коливань з параметрами електронного потоку і діода. Рішення дисперсійного рівняння показує, що в діоді, крізь який розповсюджується сповільнений електронний потік, виникає не описана раніше нестійкість коливань у СВЧ-діапазоні. Ця нестійкість має місце, коли в стаціонарному стані мінімум потенціалу в діоді не утворюється. Експериментально підтверджено виникнення нестійкості коливань з передбаченими теоретично частотами і декрементами у відповідних областях параметрів пучка і діода.